Ain Shams University

Ain Shams Engineering Journal
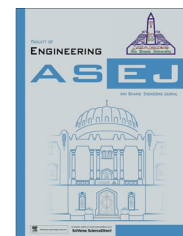
ENGINEERING PHYSICS AND MATHEMATICS

2-(4-{[4-Methyl-6-(1-methyl-1*H*-1,3-benzodiazol-2-yl)-2-propyl-1*H*-1,3-benzodiazol-1-yl] methyl} phenyl) benzoic acid as green corrosion inhibitor for mild steel in 1 M hydrochloric acid

Chandrabhan Verma, M.A. Quraishi *, Neeraj Kumar Gupta

Department of Chemistry, Indian Institute of Technology, Banaras Hindu University, Varanasi 221005, India

Abstract   Present study describes the inhibition property of benzo 1,3-diazol 2-(4-{[4-Methyl-6-(1-methyl-1*H*-1,3-benzodiazol-2-yl)-2-propyl-1*H*-1,3-benzodiazol-1-yl] methyl} phenyl) benzoic acid (Telmisartan, Cresar-H) on mild steel corrosion in 1 M HCl using weight loss, electrochemical, and surface measurements. Results showed that the corrosion inhibition efficiency ($\eta\%$) increases with increasing Telmisartan concentration and attained the maximum value of 97.39% at 125 mg L^{-1} concentration. Polarization studies revealed that Telmisartan acted as cathodic type inhibitor. Electrochemical impedance spectroscopy (EIS) studies suggested that the Telmisartan inhibits mild steel corrosion by becoming adsorbate at the metallic/electrolyte surfaces. Among the several tested isotherms, adsorption of the Telmisartan on mild steel surface obeyed the Temkin adsorption isotherm. The values of the apparent activation energy (E_a) suggested that Telmisartan inhibited metallic corrosion by creating energy barrier for corrosion process. The adsorption of corrosion inhibition was well supported by SEM/EDX and AFM studies.

1. Introduction

Iron and its alloys are widely used in different industries as construction materials due to their high mechanical strength and low cost [1,2]. However, they are highly reactive and very prone to corrosion by chemical and electrochemical reactions with the environment [3]. Several methods have been described in the literature in order to prevent these undesirable reactions. Among the available methods, the consumption of the synthetic corrosion inhibitors is one of the most economic, practical and cost effective methods [4,5]. Generally, organic

* Corresponding author. Fax: +91 542 2368428.
E-mail addresses: maquraishi.apc@itbhu.ac.in, maquraishi@rediffmail.com (M.A. Quraishi).

inhibitors inhibit metallic corrosion by adsorbing on the metal/electrolyte interfaces. The adsorption of these inhibitors was influenced by several factors such as molecular size, nature of substituents, nature of metal and electrolytic solution [6–8]. Unfortunately, most of the synthetic inhibitors used are very expensive, health hazards, toxic and non-environmental friendly [9–11]. Moreover, the increasing ecological awareness and strict environmental regulations demand green corrosion inhibitors at no or less environmental risk [12,13]. And therefore there is a demand to generate corrosion inhibitors from environmental friendly "green synthesis" and/or natural resources [14–16]. Due to their natural origin in addition to their nontoxic nature and negligible impact on the aquatic environment, drugs seem to be most ideal alternative candidate to replace these traditional toxic corrosion inhibitors [17]. Literature survey reveals that numerous chemical medicines have been used previously to prevent the metallic corrosion in different electrolytic media [18–30]. However, most of used drugs showed comparatively low corrosion inhibition efficiency at higher concentrations. The corrosion inhibition efficiency of Metformin in 1 M hydrochloric acid was investigated by Singh et al. at mild steel corrosion [31]. The authors found the maximum inhibition efficiency of 96% at 400 ppm concentration. Verma et al. [28,32] studied the inhibition efficiency of Acyclovir and Abacavir in 1 M HCl on mild steel corrosion. They found that both the drugs showed maximum inhibition efficiency of 92.6% and 97.71% efficiencies at 500 and 400 ppm concentrations, respectively. Similarly, the corrosion inhibition performance of Phenobarbital studied by Singh et al. [33] showed that investigated drug exhibited maximum inhibition efficiency of 95% at 200 ppm concentration.

Telmisartan (Cresar-H) is a commercial name of the benzo 1,3-diazol 2-(4-{[4-Methyl-6-(1-methyl-1H-1,3-benzodiazol-2-yl)-2-propyl-1H-1,3-benzodiazol-1-yl] methyl} phenyl) benzoic acid. In the present study, we investigate the inhibition efficiency of this drug on mild steel corrosion in 1 M HCl using weight loss, electrochemical impedance spectroscopy (EIS), potentiodynamic polarization, scanning electron microscopy (SEM), high energy dispersive X-ray spectroscopy (EDX) and atomic force microscopy (AFM) techniques. The drug (Telmisartan, 40 mg) marketed by Cipla Pharma Limited (India) was purchased and used in the study. The chemical formula and molecular weight of Telmisartan are $C_{33}H_{30}N_4O_2$ and 514.61, respectively. Chemical structure of the Telmisartan is shown in Fig. 1. The Telmisartan has several good features such as (i) it is a green compound and its LD_{50} is more than 2000 mg/kg for rates, (b) it possesses four nitrogen atoms of benzo diazoles rigs and two oxygen atoms of the carboxylic

acid group in addition to several aromatic rings those can act as adsorption centers, (c) it exhibits high solubility in the test solution due to the presence of carboxylic acid groups and other heteroatoms and (d) it has very large molecular size and therefore should effectively inhibit metallic corrosion. The presence of these salient properties of Telmisartan that facilitate the adsorption on the metallic surface, the Telmisartan has been chosen as corrosion inhibitor in the present study.

2. Experimental procedures

2.1. Materials

The mild steel specimens with percentage chemical composition: C (0.076), Mn (0.192), P (0.012), Si (0.026), Cr (0.050), Al (0.023), and Fe (balance) were used for all weight loss, electrochemical and surface studied. Before exposing the specimens into the test solution, they were cleaned by emery papers of SiC having different grades ranging from 600 to 1200 mesh size, then washed with double distilled water, degreased with acetone, and collected in desiccator. The test solution of 1 M HCl was prepared on diluting analytical grade HCl (37%) purchased from MERCK, India, by double distilled water.

2.2. Methods

2.2.1. Weight loss measurements

The cleaned and accurately weighted mild steel specimens of dimension $2.5 \times 2.0 \times 0.025$ cm^3 with above mentioned chemical composition were immersed in 100 mL of 1 M HCl for 3 h in the absence and presence of different concentrations of Telmisartan. After, elapsed of time, the specimens were taken out, washed and weighted. Each experiment was triply performed in order to insure the reproducibility. The percentage inhibition efficiency ($\eta\%$) was calculated from the derived weight loss in the absence and presence of Telmisartan using following relation [34,35]:

$$\eta\% = \frac{w_o - w_i}{w_o} \times 100 \tag{1}$$

where w_0 and w_i are the weight loss values in the absence and presence of Telmisartan at different concentrations, respectively.

2.2.2. Electrochemical measurements

Gamry Potentiostat/Galvanostat (Model G-300) instrument having Gamry Echem Analyst 5.0 software for fitting and analyzing all electrochemical data was used to carry out all electrochemical measurements. The instrument consists of conventional three electrode glass cell assembly in which mild steel specimen acts as working electrode, pure platinum foil acts as counter electrode and saturated calomel acts as reference electrode. The mild steel specimens were allowed to corrode free in the absence and presence of Telmisartan for 30 min before starting the electrochemical experiments in order to establish the open circuit potential (OCP). The potentiodynamic polarization studied were performed by inevitably changing the electrode potential from 0.25 to +0.25 V vs. corrosion potential (E_{corr}) at a constant sweep rate of 1.0 mV s^{-1}. The extrapolation of the anodic and cathodic Tafel curves
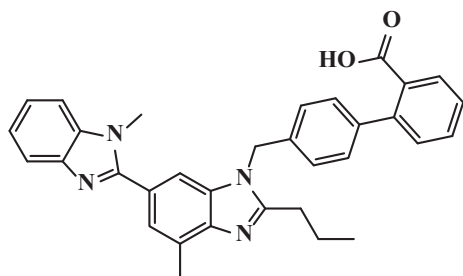

Figure 1   Chemical structure of Telmisartan.

gives the values of corrosion current densities in the absence and presence of Telmisartan. The percentage corrosion inhibition efficiency was calculated using following relation [34,35]:

$$\eta\% = \frac{i_{corr}^0 - i_{corr}^i}{i_{corr}^0} \times 100 \qquad (2)$$

where i_{corr} and i_{corr} are corrosion current in the absence and presence of Telmisartan, respectively.

The electrochemical impedance measurements in the absence and presence of Telmisartan were carried at open circuit potential in the frequency range of 100 kHz to 0.01 Hz using AC signal of amplitude 10 mV peak to peak. The values of charge transfer resistances (R_{ct}) were derived from Nyquist plots by using which percentage inhibition efficiency was calculated using following relationship [34,35]:

$$\eta\% = \frac{R_{ct}^i - R_{ct}^0}{R_{ct}^i} \times 100 \qquad (3)$$

where R_{ct}^0 and R_{ct}^i are charge transfer resistances in the absence and presence of Telmisartan, respectively.

2.2.3. SEM, EDX and AFM measurements

The mild steel specimens were allowed to corrode in 1 M HCl for 3 h in the absence and presence of optimum concentration of Telmisartan. After 3 h, mild steel specimens were taken out, washed with distilled water, and dried and their surface morphology studies were carried out by SEM, EDX, and AFM methods. For SEM analysis, the Ziess Evo 50 XVP model was used and scanning magnification was 500×. The elements present on the metallic surface were studied by an EDX detector jointed to the SEM. For AFM analysis, NT-MDT multimode AFM, Russia, 111 controlled by solvers canning probe microscope controller was used. The single beam cantilever having resonance frequency in the range of 240–255 kHz in semi contact mode with corresponding spring constant of 11.5 N/m with NOVA program was used for image interpretation. The scanning area during AFM analysis was 5 mm × 5 mm.

3. Results and discussions

3.1. Weight loss measurements

3.1.1. Effect of Telmisartan concentration

Due to its simplicity and good reliability, the corrosion inhibition property of Telmisartan was first studied by weight loss experiment. Variation of the inhibition efficiency with Telmisartan concentrations is shown in Fig. 2a and various weight loss parameters are given in Table 1. Inspection of the results shows that the inhibition efficiency increases on increasing Telmisartan concentration from 25 to 125 mg L^{-1} concentration, and further increase in concentration did not cause any significant change in the inhibition performance suggesting that 125 mg L^{-1} is the optimum concentration. The increase in Telmisartan concentration increases the surface coverage (θ) through adsorbing on mild steel surface and therefore, increases inhibition efficiency [36]. It has been reported that increase in the inhibitor concentrations increases the surface coverage which results into increase in the inhibition performance [37,38]. However, after a particular (optimum) concen-
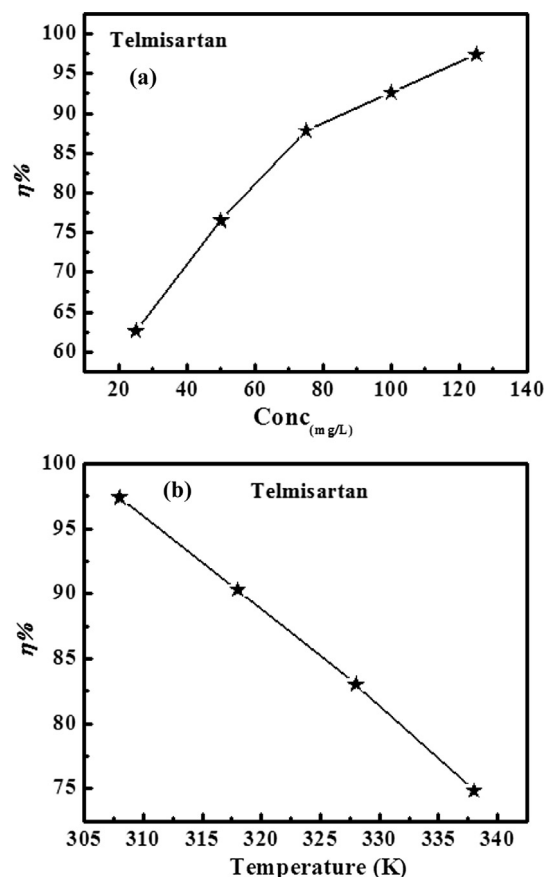
Figure 2 (a) Variation of inhibition efficiency with Telmisartan concentration, (b) variation of inhibition efficiency with solution temperature.

Table 1 The weight loss parameters obtained for mild steel in 1 M HCl containing different concentrations of Telmisartan.

Inhibitor	Conc (mg L^{-1})	Weight loss (mg)	θ	$\eta\%$
Blank	0.0	230	–	–
Telmisartan	25	86	0.6260	62.60
	50	54	0.7652	76.52
	75	28	0.8782	87.82
	100	17	0.9260	92.60
	125	6	0.9739	97.39

tration further increase in the inhibitor concentration did not cause any significant enhancement in the inhibition performance which could be possible as a result of no significant increase in the metallic surface coverage after optimum concentration, where the maximum surface coverage already occurs [39]. The high inhibition efficiency of Telmisartan is attributed due to large molecular size, the presence of several aromatic rings and heteroatoms (N, O) which influenced the adsorption of the drug on mild steel surface.

3.1.2. Effect of solution temperature

Variation of the inhibition efficiency with solution temperature ranging from 308 to 338 K is shown in Fig. 2b. It can be seen

from the figure that $\eta\%$ decreases on increasing solution temperature. This decrease in the $\eta\%$ at elevated temperature is attributed due to several phenomenons such as increase in kinetic energy of the Telmisartan which decreases the attraction between adsorbate and adsorbent and/or decomposition of inhibitor. The effect of temperature on the $\eta\%$ of the Telmisartan on mild steel corrosion can be best explained in term of Arrhenius equation, where the natural logarithm of C_R is a linear function of $1/T$ [40]:

$$\log(C_R) = \frac{-E_a}{2.303RT} + \log A \tag{4}$$

where C_R is the corrosion rate in mg cm^{-2} h^{-1}, A is the Arrhenius pre-exponential factor, R is the gas constant, T is absolute temperature and E_a is the apparent activation energy. The values of E_a were calculated from the slope of Arrhenius plots ($-\Delta E_a/2.303R$) (Fig. 3) in the absence and presence of Telmisartan and given in Table 2. From the results shown in Table 2 it can be seen that value of apparent activation energy (E_a) in the presence of Telmisartan is much higher (95.65 kJ mol^{-1}) as compared to in its absence (28.48 kJ mol^{-1}) suggesting that in the presence of Telmisartan, the corrosion process becomes more difficult and requires high energy due to formation of protective film by Telmisartan at metal/electrolyte interfaces [41].

3.1.3. Adsorption isotherm and adsorption consideration

Adsorption of inhibitor on metallic surface is one of the most important topics in the corrosion study because it provides significant information about electric double layer as well as thermodynamic nature of the metallic corrosion. In our present study, in order to clarify the nature and strength of adsorption, Langmuir, Temkin and Frumkin isotherms were tested. These isotherms can be best represented by following relations [42]:

$$\text{Langmuir}: \ \theta/(1-\theta) = K_{ads}C_{inh} \tag{5}$$
$$\text{Temkin}: \ \log(\theta/C_{inh}) = \log K_{ads} - g\theta \tag{6}$$
$$\text{Frumkin}: \ \log(\theta/(1-\theta)C_{inh}) = \log K_{ads} + g\theta \tag{7}$$

where θ is the surface coverage, K_{ads} is the equilibrium constant for adsorption-desorption processes, C_{inh} is the Telmisartan concentration and g is the adsorbate interaction
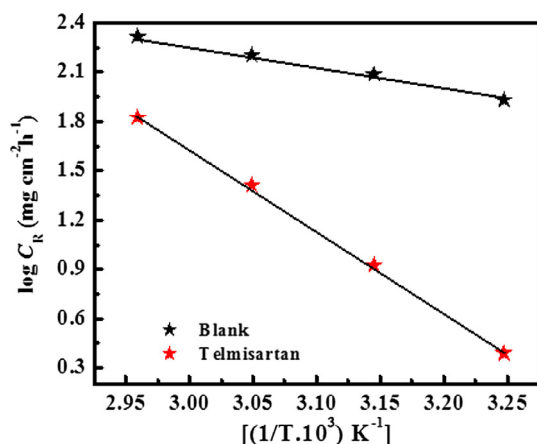
Table 2 Values of apparent activation energies in the absence and presence of optimum concentration of Telmisartan.

Inhibitor	E_a (kJ mol^{-1})
Blank	28.48
Telmisartan	95.64

parameter. Among the tested adsorption isotherm (Fig. 4), the Temkin isotherm gave the best fit with value of regression coefficient very close to unity. The criterion behind selection of best isotherm was the values of regression coefficient (R^2). The values of regression coefficients (R^2) were 0.9126, 0.9216 and 0.9996 for Langmuir, Frumkin, and Temkin isotherm, respectively. The Temkin isotherm gave a straight line between log C_{inh} and surface coverage (θ), from the intercept of which values of K_{ads} were calculated. The standard free energy of adsorption (ΔG_{ads}^0), is related to the K_{ads} by the equation [43]:

$$\Delta G_{ads}^o = -RT\ln(55.5K_{ads}) \tag{8}$$

In the above equation, the numerical value 55.5 represents the molar concentration of water in acid solution. The calculated values of K_{ads} and ΔG_{ads}^0 at each studied temperature in the presence of optimum concentration of Telmisartan are given in Table 3. Literature study reveals that the value of ΔG_{ads}^0 up to -20 kJ mol^{-1} or less negative is related to the electrostatic interactions between inhibitor and metallic surfaces (physisorption), while the value of ΔG_{ads}^0 is around -40 kJ mol^{-1} or more negative related to the charge sharing between inhibitor and metallic surfaces (chemisorption) [44]. However, in our present case the values of ΔG_{ads}^0 range in between -34.28 and -37.72 kJ mol^{-1} suggesting that adsorption of the Telmisartan on mild steel surface follows physiochemisorption (mixed mode of adsorption) [45,46].

3.2. Electrochemical measurements

3.2.1. Potentiodynamic polarization studies

The potentiodynamic polarization nature of Telmisartan on mild steel corrosion in 1 M HCl is shown in Fig. 5 and polarization parameters such as corrosion potential (E_{corr}), corrosion current density (i_{corr}), anodic and cathodic Tafel slopes (β_a, β_c) and corresponding inhibition efficiency ($\eta\%$) were calculated from extrapolation of linear segments of the anodic and cathodic Tafel curves and given in Table 4. From the results depicted in Table 4 it can be seen that values of corrosion current density (i_{corr}) for mild steel in 1 M HCl decreased with increase in Telmisartan concentration. This decrease in i_{corr} values might be attributed due to adsorption of the Telmisartan at metal/electrolyte interfaces and therefore, it can be concluded that Telmisartan inhibits mild steel corrosion by adsorbing on the mild steel surface which isolates the metal from aggressive acid solution [47,48]. Moreover, the maximum shift in the value of E_{corr} in the present study was 66 mV which is less than 85 mV. Therefore, the Telmisartan can be classified as mixed-type inhibitor, which implies the inhibitor reduces the anodic mild steel dissolution and also retards the cathodic hydrogen evolution reaction [47,48]. Moreover, from the results depicted in Table 4 it can be observed that in the presence of Telmisartan at different concentrations the values of β_a

Figure 3 Arrhenius plot for mild steel dissolution in 1 M HCl.
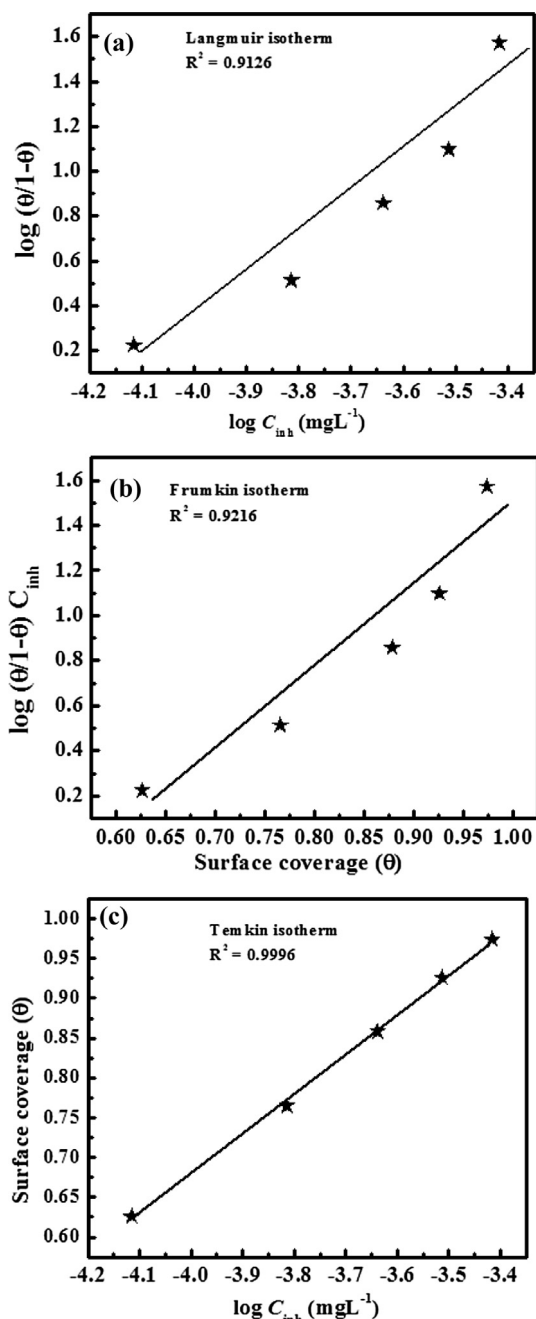
Figure 4 (a) Langmuir, (b) Frumkin and (c) Temkin adsorption isotherm plots for the adsorption of Telmisartan on the surface of mild steel.

and β_c change as compared to in free acid solution. However, the shifts in values of β_c were more prominent as compared to shift in β_a suggesting that Telmisartan acts as predominantly cathodic type inhibitor [47,48].

3.2.2. Electrochemical impedance spectroscopy (EIS) studies

Fig. 6a represents the Nyquist plots for mild steel corrosion in the absence and presence of different concentrations of Telmisartan after 30 min immersion time. It can be seen from the figure that Nyquist plots consist of single semicircle capacitive loop which corresponds to one time constant in Bode plots (Fig. 6b). This finding suggests that corrosion of mild steel in 1 M HCl is mainly controlled by a charge transfer process [49]. Some common impedance parameters such as solution resistance (R_s), charge transfer resistance (R_{ct}), phase shift (n), double layer capacitance (C_{dl}), surface coverage (θ) and inhibition efficiency ($\eta\%$) were calculated using equivalent circuit model described elsewhere [50] and given in Table 5. The equivalent circuit model consists of a CPE, (R_{ct}), and (R_s). The impedance (Z_{CPE}) of the CPE can be expressed using following relations [51]:

$$Z_{CPE} = \left(\frac{1}{Y_0}\right)[(j\omega)_n]^{-1} \qquad (9)$$

where Y_0 is the amplitude comparable to a capacitance (with a $\mu F\ cm^{-2}$), j is the square root of -1, ω is angular frequency ($\omega = 2\pi f_{max}$) at which the imaginary part of the impedance ($-Z_{im}$) is maximal and f_{max} is AC frequency at maximum, and n is the phase shift. Generally, the value of n equals to 0, 1, -1 and 0.5 associated with the resistance, capacitance, inductance and Warburg impedance nature of the metal/electrolyte interface, respectively. From the results depicted in Table 5 it can be seen that values of n vary from 0.857 to 0.869. In our present study values of C_{dl} with and without Telmisartan were calculated using following equation [52]:

$$C_{dl} = \frac{Y\omega^{n-1}}{\sin(n(\pi/2))} \qquad (10)$$

Inspection of the results shown in Table 5 suggests that values of C_{dl} decreased and values of R_{ct} increased in the presence of the Telmisartan. Furthermore, this decrease in C_{dl} and increase in R_{ct} values are more pronounced at higher Telmisartan concentrations. The decreased value of C_{dl} in the presence of Telmisartan is due to the decrease in local dielectric constant and/or an increase in the thickness of the electrical double layer [53–55]. The increase in R_{ct} values in the presence of Telmisartan is credited due to formation of protective film at the metal/solution interface by Telmisartan [53–55]. This finding suggests that Telmisartan inhibits mild steel corrosion in 1 M HCl by protective surface film at metal/electrolyte interfaces.

3.3. Surface measurements

3.3.1. SEM/EDX studies

SEM micrographs in the absence and presence of optimum concentration of the Telmisartan after 3 h immersion time and corresponding EDX spectra are shown in Figs. 7 and 8.

Table 3 Values of $-\Delta G°_{ads}$ and K_{ads} for mild steel in 1 M HCl at different temperatures.

| Inhibitor	K_{ads} ($10^4\ M^{-1}$)				$-\Delta G°_{ads}$ (kJ mol^{-1})			
	308	318	328	338	308	318	328	338
Telmisartan	4.47	1.11	0.58	0.35	37.72	35.27	34.62	34.28
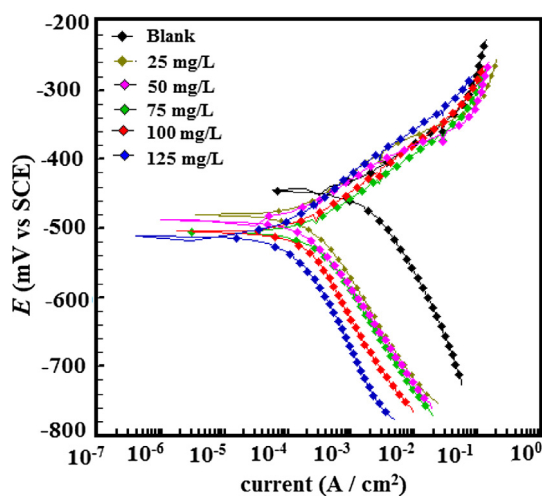
Figure 5 Tafel polarization curves for corrosion of mild steel in 1 M HCl in the absence and presence of different concentrations of Telmisartan.

Fig. 7a represents the SEM micrograph of the mild steel surface immersed in 1 M HCl without Telmisartan which seems to be highly corroded and damaged due to free acid attack. However, in the presence of optimum concentration of the Telmisartan in acid solution causes significant improvement in the surface morphology. Therefore, it is concluded that Telmisartan forms protective surface film through adsorption which isolates the metal from aggressive acid solution responsible for improvement in the surface morphology. Further, adsorption mechanism of corrosion inhibition is supported by EDX spectra of mild steel surface taken in the absence and presence of the Telmisartan. Fig. 8a shows the EDX spectrum of mild steel specimen immersed in 1 M HCl in the absence of the Telmisartan which is characterized by signals corresponding only for C, O and Fe. However, EDX spectrum in the presence of Telmisartan shows additional signal for nitrogen (N) which is attributed due to adsorption of Telmisartan on mild steel surface. Moreover, signal intensity for oxygen (O) is high in the presence of Telmisartan as compared to in its absence which is attributed again due to adsorption of the Telmisartan on the metallic surface.

3.3.2. AFM studies

Fig. 9 represents the AFM surface morphology of the mild steel specimens immersed in 1 M HCl for 3 h solutions without and with optimum concentration of the Telmisartan. It can be seen from the AFM micrograph of the mild steel specimen in
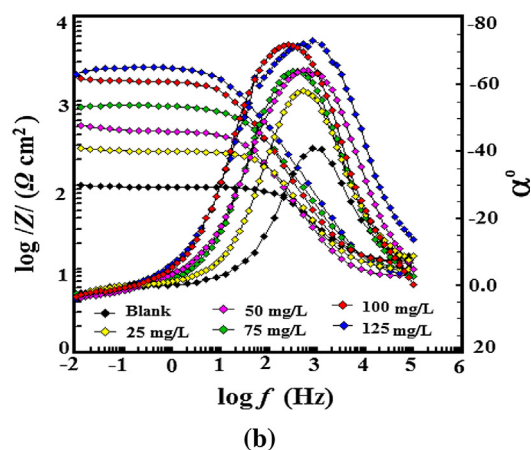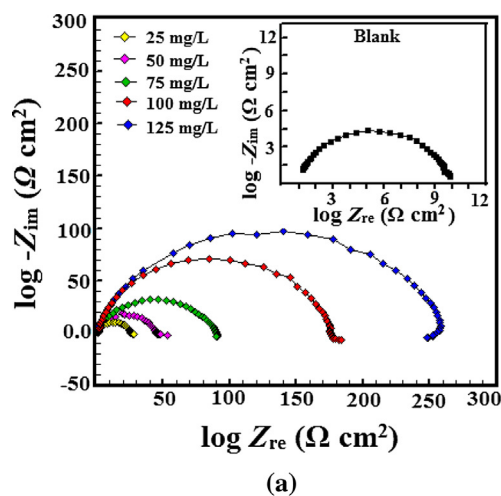

Figure 6 (a) Nyquist and (b) plots of mild steel in 1 M HCl in the absence and presence of different concentrations of Telmisartan.

the absence of Telmisartan (Fig. 9a) that the surface showed a very irregular topography and mountain like appearance with highly corroded and damaged surface due to corrosive attack of acid. The calculated surface roughness in the absence of the Telmisartan was 392 nm. However, in the presence of optimum concentration of the Telmisartan (Fig. 9b), the surface morphology is remarkably improved due to formation protective film by Telmisartan at metal electrolyte interfaces. The calculated surface roughness of mild steel specimen in the presence of Telmisartan was 172 nm.

Table 4 The values of polarization parameters for mild steel dissolution in the absence and presence of different concentrations of Telmisartan.

Inhibitor	Conc (mg L^{-1})	E_{corr}	β_a	$-\beta_c$	i_{corr}	$\eta\%$	θ
Blank	–	−445	70.5	114.6	1150	–	–
Telmisartan	25	−505	73.40	135.2	446.0	61.21	0.6121
	50	−481	79.80	131.6	274.0	76.17	0.7617
	75	−505	75.40	165.8	149.0	87.04	0.8704
	100	−488	59.10	134.9	68.3	94.06	0.9406
	125	−511	49.80	132.3	26.8	97.66	0.9766
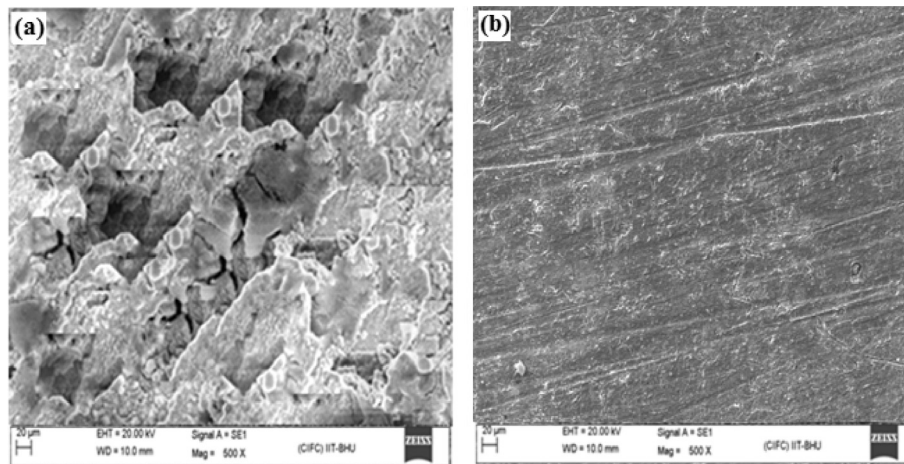
Figure 7   SEM micrographs for mild steel surface (a) in the absence and (b) in the presence of Telmisartan.
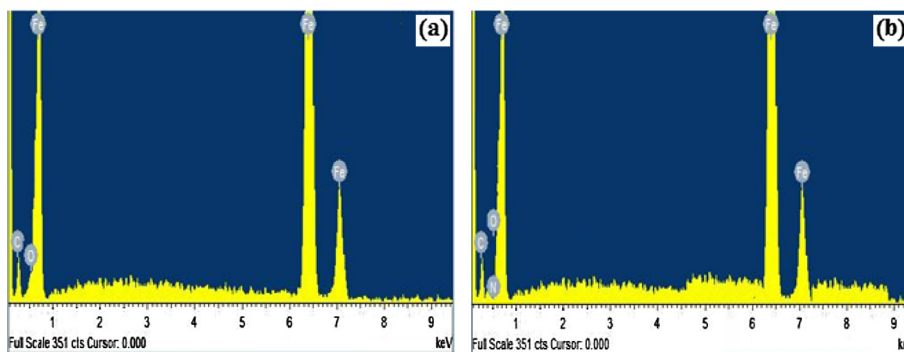

Figure 8   EDX spectra of mild steel surface (a) in the absence and (b) in presence of Telmisartan.

Table 5   EIS parameters obtained for mild steel in 1 M HCl in without and with different concentrations of Telmisartan.

Inhibitor	Conc (mg L^{-1})	R_s	R_{ct}	C_{dl}	n	$\eta\%$
Blank	–	1.12	9.58	106.21	0.827	–
Telmisartan	25	0.997	24.96	112.76	0.859	61.61
	50	0.822	44.56	104.31	0.869	78.50
	75	0.963	86.98	59.13	0.857	88.98
	100	1.142	175.4	50.81	0.863	94.53
	125	0.747	246.9	45.71	0.862	96.11

4. Mechanism of inhibition

It has been established that the inhibitor molecule containing heteroatoms particularly nitrogen, sulfur, oxygen and phosphorus inhibits metallic corrosion in acid solution by adsorbing at the metal/electrolyte interfaces. Previously, it has been investigated by several authors [56–58] that heteroatoms of the inhibitor molecule in acid solution easily undergo protonation due to the presence of unshared electron pair on these atoms, and therefore in acid solution organic compounds exist in cationic form. On the other hand the metallic surface becomes negatively charged due to the presence of uniform layer counter ion (chloride ions of hydrochloric acid) present over the metallic surface [56–58]. These appositively charged
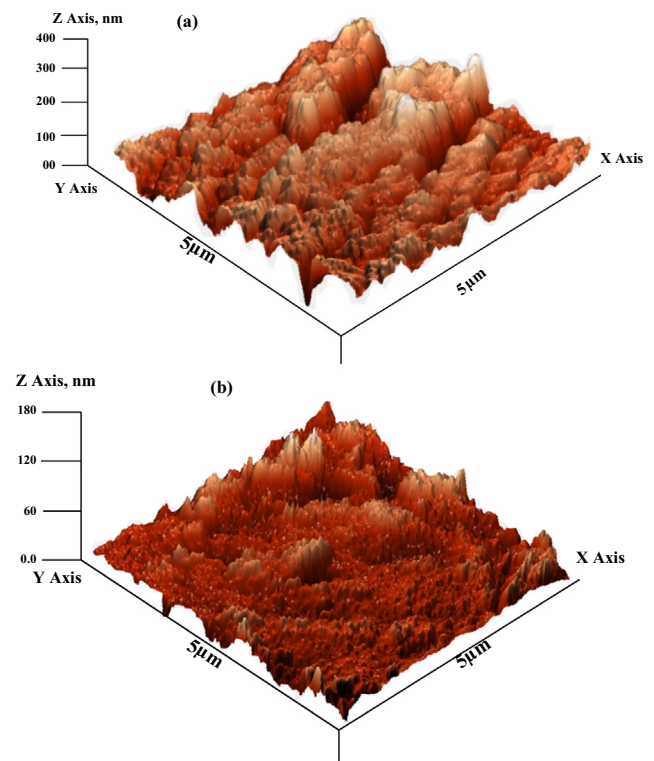
Figure 9   AFM micrographs for mild steel surface (a) in the absence and (b) in the presence of optimum concentration of Telmisartan.
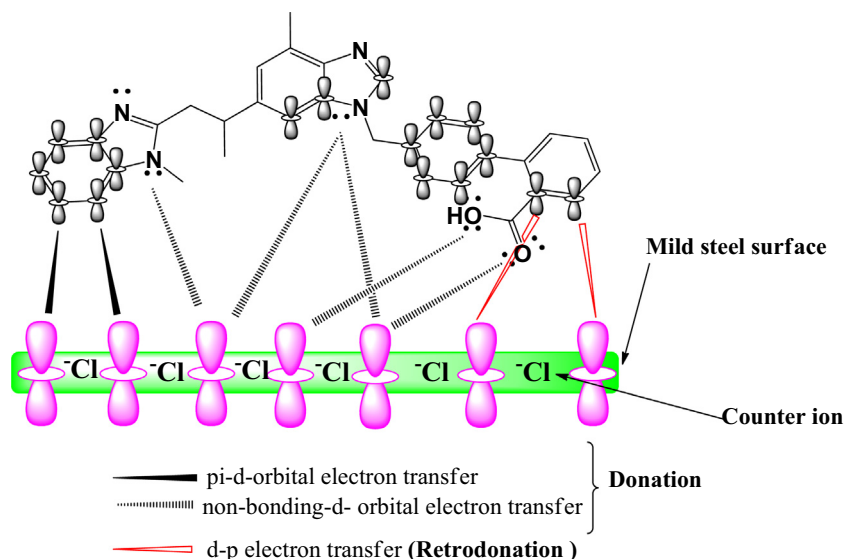
Figure 10 Pictorial presentation of adsorption of Telmisartan on mild steel surface in acid solution.

species attracted each other through electrostatic force of attraction, and therefore it can be concluded that first step involves physisorption during the inhibitor adsorption processes [56–58]. However, as soon as inhibitor comes in its neutral form by release of hydrogen gas at cathode, the chemisorption takes place by transfer of free unshared electron pairs of heteroatoms into empty d-orbitals of surface iron atoms [59]. Moreover, this type of electron transfer causes excessive accumulation of negative charge on electron rich metallic surface which renders it to transfer its electrons to the empty anti-bonding molecular orbitals of the inhibitors through retro-donation. The interaction between metal and inhibitor molecule may occur by following ways: (a) electrostatic interaction between appositively charged inhibitor and metallic surface; physisorption (b) interaction with unshared electron pairs of heteroatoms d-orbital of surface Fe atoms; chemisorption (donation) (c) interaction between pi-electrons of the inhibitor molecules with d-orbitals of the surface Fe atoms; chemisorption (donation) and (d) transfer of electron from d-orbitals of surface Fe atoms to empty anti-bonding molecular orbitals of the inhibitor molecule, retro-donation; chemisorption [59,60]. This donation and retro-donation strengthen each other through a phenomenon of synergism [60]. The pictorial presentation depicting several modes of adsorption of investigated inhibitor molecule on the mild steel surface is shown in Fig. 10.

5. Conclusion

From the above study it can be concluded that benzo 1,3-diazol 2-(4-{[4-Methyl-6-(1-methyl-1*H*-1,3-benzodiazol-2-yl)-2-propyl-1*H*-1,3-benzodiazol-1-yl] methyl} phenyl) benzoic acid (Telmisartan, Cresar-H) acts as good corrosion inhibitor. The corrosion inhibition efficiency increases with increasing Telmisartan concentration and decreases with increasing solution temperature. Adsorption of the Telmisartan on the mild steel surface obeyed the Temkin isotherm. Polarization study revealed that Telmisartan acted as mixed type but predominantly cathodic inhibitor. EIS studies revealed that the studied drug formed a protective surface film at metal/electrolyte interfaces.

References

[1] Zhang K, Xu B, Yang W, Yin X, Liu Y, Chen Y. Corros Sci 2015;90:284–95.

[2] Singh P, Quraishi MA, Gupta SL, Dandia A. J Taibah Univ Sci 2016;10:139–47.

[3] Farag AA, Ali TA. J Ind Eng Chem 2015;21:627–34.

[4] Hasanov R, Bilge S, Bilgiç S, Gece G, Kılıç Z. Corros Sci 2010;52:984–90.

[5] Verma C, Singh P, Bahadur I, Ebenso EE, Quraishi MA. J Mol Liq 2015;209:767–78.

[6] Ahamad I, Prasad R, Ebenso Eno E, Quraishi MA. Int J Electrochem Sci 2012;7:3436–52.

[7] Yurt Aysel, Duran Berrin, Dal Hakan. Arab J Chem 2014;7:732–40.

[8] Verma C, Olasunkanmi LO, Obot IB, Ebenso EE, Quraishi MA. RSC Adv 2016;6:53933–48.

[9] Winkler DA, Breedon M, Hughes AE, Burden FR, Barnard AS, Harvey TG, Cole I. Green Chem 2014;16:3349–57.

[10] Geethamani P, Kasthuri PK. Cogent Chem 2015;1:1091558.

[11] Al-Amiery AA, Kassim FAB, Kadhum AAH, Mohamad AB. Sci Rep 2016;6:1–13.

[12] Verma C, Ebenso EE, Olasunkanmi LO, Quraishi MA, Obot IB. J Phys Chem C 2016;120:11598–611.

[13] Abiola OK, Otaigbe JOE, Kio OJ. Corros Sci 2009;51:1879–81.

[14] Kadhum AAH, Mohamad Abu Bakar, Hammed Leiqaa A, Al-Amiery Ahmed A, San N Hooi, Musa Ahmed Y. Materials 2014;7:4335–48.

[15] Al-Amiery AA, Kadhum AAH, Mohamad AB, Junaedi Sutiana. Materials 2013;6:1420–31.

[16] Al-Amiery AA, Kadhum AAH, Alobaidy AHM, Mohamad AB, Hoon PS. Materials 2014;7:662–72.

[17] Gece G. Corros Sci 2011;53:3873–98.

[18] Shahi G, Verma C, Ebenso EE, Quraishi MA. Int J Electrochem Sci 2015;10:1102–16.

[19] Shukla SK, Quraishi MA. Mater Chem Phys 2010;120:142–7.

[20] Eddy NO, Odoemelam SA, Ekwumemgbo P. Sci Res Essays 2009;4:33–45.

[21] Ahamad I, Prasad R, Quraishi MA. J Solid State Electrochem 2010;14:2095–105.
[22] Al-Shafey HI, Hameed RSA, Ali FA, el-Aleem A, Aboul-Magd S, Salah M. Int J Pharm Sci Rev Res 2014;27:146–52.
[23] Shukla SK, Quraishi MA, Ebenso Eno E. Int J Electrochem Sci 2011;6:2912–31.
[24] Ade Suraj B, Shitole NV, Lonkar SM. Int J ChemTech Res 2014;6:3642–50.
[25] Eddy NO, Ibok UJ, Ebenso Eno E, El Nemr A, El Ashry ESH. J Mol Mod 2009;15:1085–92.
[26] Reddy MJ, Verma C, Ebenso EE, Singh KK, Quraishi MA. Int J Electrochem Sci 2014;9:4884–99.
[27] Shukla SK, Quraishi MA. Corros Sci 2009;51:1007–11.
[28] Verma C, Quraishi MA, Ebenso EE. Int J Electrochem Sci 2013;8:7401–13.
[29] Singh A, Singh AK, Quraishi MA. Open Electrochem J 2010;2:43–51.
[30] Verma C, Quraishi MA, Singh A. J Taibah Univ Sci 2016. http://dx.doi.org/10.1016/j.jtusci.2015.10.005.
[31] Singh A, Ebenso Eno E, Quraishi MA. Int J Electrochem Sci 2012;7:4766–79.
[32] Verma C, Quraishi MA, Ebenso EE. Int J Electrochem Sci 2013;8:12238–51.
[33] Singh A, Pramanik T, kumar A, Gupta M. Asian J Chem 2013;25:9808–12.
[34] Verma C, Singh Pooja, Quraishi MA. J Assoc Arab Univ Basic Appl Sci 2015. http://dx.doi.org/10.1016/j.jaubas.2015.04.003.
[35] Verma CB, Reddy MJ, Quraishi MA. Anal Bioanal Electrochem 2014;6:515–34.
[36] Yadav M, Behera D, Kumar S, Sinha RR. Ind Eng Chem Res 2012;52:6318–28.
[37] Elmsellem H, Nacer H, Halaimia F, Aouniti A, Lakehal I, Chetouani A, Al-Deyab SS, Warad I, Touzani R, Hammouti B. Int J Electrochem Sci 2014;9:5328–51.
[38] Elmsellem H, Elyoussfi A, Steli H, Sebbar NK, Essassi EM, Dahmani M, El Ouadi Y, Aouniti A, El Mahi B, Hammouti B. Der Pharma Chemica 2016;8:248–56.
[39] Elmsellem H, Aouniti A, Youssoufi MH, Bendaha H, Ben hadda T, Chetouani A, Warad I, Hammouti B. Phys Chem News 2013;70:84–90.
[40] Verma C, Singh A, Pallikonda G, Chakravarty M, Quraishi MA, Bahadur I, Ebenso EE. J Mol Liq 2015;209:306–19.
[41] Verma C, Quraishi MA, Singh A. J Mol Liq 2015;212:804–12.
[42] de Souza FS, Spinelli A. Corros Sci 2009;51:642–9.
[43] Verma C, Quraishi MA, Ebenso EE, Obot IB, El Assyry A. J Mol Liq 2016;219:647–60.
[44] Amin MA, Ibrahim MM. Corros Sci 2011;53:873–85.
[45] Verma C, Olasunkanmi LO, Obot IB, Ebenso EE, Quraishi MA. RSC Adv 2016;6:15639–54.
[46] Chakib I, Elmsellem H, Sebbar NK, Lahmidi S, Nadeem A, Essassi EM, Ouzidan Y, Abdel-Rahman I, Bentiss F, Hammouti B. J Mater Environ Sci 2016;7:1866–81.
[47] Murulana LC, Kabanda MM, Ebenso EE. RSC Adv 2015;5:28743–61.
[48] Alkhathlan HZ, Khan M, Abdullah MMS, AlMayouf AM, Yacine Badjah-Hadj-Ahmed A, AlOthman ZA, Mousa AA. RSC Adv 2015;5:54283–92.
[49] Xu B, Ji Y, Zhang X, Jin X, Yang W, Chen Y. RSC Adv 2015;5:56049–59.
[50] Gupta NK, Verma C, Quraishi MA, Mukherjee AK. J Mol Liq 2016;215:47–57.
[51] Verma C, Singh A, Quraishi MA. J Taiwan Inst Chem Eng 2015. http://dx.doi.org/10.1016/j.jtice.2015.06.020.
[52] Yousefi A, Javadian S, Dalir N, Kakemam J, Akbari J. RSC Adv 2015;5:11697–713.
[53] Verma CB, Quraishi MA, Singh A. J Taiwan Inst Chem Eng 2015;49:229–39.
[54] Elmsellem H, Basbas N, Chetouani A, Aouniti A, Radi S, Messali M, Hammouti B. Portugaliae Electrochim Acta 2014;3:77–108.
[55] Verma C, Quraishi MA, Olasunkanmi LO, Ebenso EE. RSC Adv 2015;5:85417–30.
[56] Obot IB, Obi-Egbedi NO, Umoren SA. Corros Sci 2009;51:276–82.
[57] Deng S, Li X, Xie X. Corros Sci 2014;80:276–89.
[58] Yadav DK, Maiti B, Quraishi MA. Corros Sci 2010;52:3586–98.
[59] Singh P, Singh A, Quraishi MA. J Taiwan Inst Chem Eng 2015:1–14.
[60] Yadav DK, Quraishi MA. Ind Eng Chem Res 2012;51:14966–79.

Chandrabhan Verma is research Scholar in Department of chemistry, IIT (BHU) Varanasi (India). I obtained B.Sc. (2007) and M.Sc. (2010) degrees from Purvanchal University (UP College). Also, I have published several research papers in the referred international journals in the field of corrosion.

M.A. Quraishi is professor in Department of chemistry, IIT (BHU) Varanasi (India). I obtained B.Sc. (1969) degree and M.Sc. (1971) degree from Saugar University, M. Phil (1978) and Ph.D (1986) from Kurukshetra University, and D.Sc. (2004) from centrally funded AMU Aligarh. Before joining as Professor at BHU, I was Reader (1990–2005) at AMU Aligarh. I have published a number of papers in different reputed journals. Also, I have published several research papers in the referred international journals and many papers in national/international conferences.

Neeraj Kumar Gupta is research Scholar in Department of chemistry, IIT (BHU) Varanasi (India). I obtained B. Tech and M. Tech degrees from IIT (BHU). Also, I have published few research papers in the referred international journals in the field of corrosion.